Break-up of self-guided light beams into X wave trains

Miguel A. Porras , Alberto Parola
Departamento de Física Aplicada, Universidad Politécnica de Madrid, Rios Rosas 21, ES-28003, Spain
CNISM and Department of Physics, University of Insubria, Via Valleggio 11, IT-22100 Como, Italy

Relaxation of the nonlinear spatiotemporal dynamics of cylindrically symmetric Schrödinger solitons due to their temporal modulation instability leads to soliton break-up into a train of X waves.

In recent years, the interest in conical waves is drifting from its original field in linear optics towards nonlinear optics The nonlinear generation of conical waves is a fascinating problem where these two fields intersect, and where temporal and spatial wave dynamics are inextricably united. X waves have been observed to emerge from focused waves in second harmonic-generating media and in self-focusing Kerr media, where their dynamics can explain many aspects of the complex spatiotemporal dynamics of light filaments. A number of mechanisms have been pointed out as responsible for the formation of the X waves, as the three wave and four wave mixing models, though it is also commonly believed that some type of wave instability is at work in their generation.

Previous works have investigated X wave instability mediated by plane waves, and the X wave dressing of spatiotemporal localized (nonlinear) sources We note here that in the experiments and simulations the wave decaying into conical waves is always strongly localized in the two transverse dimensions, and that the X waves represent the last, or relaxation stage of the wave dynamics. In this Letter we then consider self-guided light beams in two transverse dimensions, or spatial solitons, supported by the nonlinear Schrödinger equation (NSE), and show that the linear relaxation of the soliton spatiotemporal dynamics triggered by its temporal modulation instability (MI) involves the formation of conical waves. As an example we consider the solitons sustained by a saturable Kerr medium with normal dispersion, and show that the soliton breaks-up into a train of X waves that emerges exponentially and represents the last stage of the evolution.

The envelope of the monochromatic, cylindrically symmetric, self-guided light beam $E = A_s \exp(-i\omega_0 t + ik_0 z)$ is a solution of the form $A_s = a(r)\exp(i\alpha z)$ of the NSE

$$\partial_z A = \frac{i}{2k_0}\Delta_\perp A - \frac{ik_0''}{2}\partial_\tau^2 A + f(|A|^2)A\,, \qquad (1)$$

or $\partial_z A = \mathcal{L}(A) + f(|A|^2)A$ for short. Above, α is a nonlinear wave vector shift, $r = (x^2+y^2)^{1/2}$, $\Delta_\perp = (1/r)\partial_r(r\partial_r)$, z is the propagation direction, $\tau = t - k_0' z$ is the local time, $k_0^{(n)} = d^{(n)}k/d\omega^{(n)}|_{\omega_0}$ characterizes the linear dispersive properties of the medium, and $f(|A|^2)$ is the soliton-supporting nonlinearity (e.g., $f(|A|^2) = ig|A|^2$, $g>0$ for self-focusing Kerr nonlinearity).

Spatial solitons suffer generally from temporal instability for a range of modulation frequencies. According to standard MI analysis in the small perturbation limit (or linear regime), this means that there exist perturbations, of the general form

$$\delta A = \epsilon\left[u(r)e^{-i\Omega_s\tau}e^{i\kappa z} + v^\star(r)e^{i\Omega_s\tau}e^{-i\kappa^\star z}\right]e^{i\alpha z}\,, \qquad (2)$$

where $\kappa_I \equiv \mathrm{Im}\kappa < 0$ and Ω_s is the modulation frequency, that can grow exponentially along z with gain $-\kappa_I$ on the top of the soliton. The eigenvalue κ, and the functions u and v are such that the complete envelope $A_s + \delta A$ satisfies the NSE in the asymptotic limit of small ϵ. Temporal MI of spatial solitons in the small perturbation regime has been studied in a number of cases, for the ground state of the cubic NSE with one transverse dimension, or for quadratic solitons, leading to neck- and snake-type instabilities. Fewer studies deal with the cylindrically symmetric case, for solitons with saturable nonlinearity, or for the Townes beam.

To our purposes, it is important to note that $A = A_s + \delta A$, i.e., the self-guided beam plus a single unstable perturbation at modulation frequency Ω_s, satisfies, when regarded as a function of z, τ and ϵ, the relation

$$\partial_z A = i\alpha A - \kappa_I \epsilon\partial_\epsilon A - (\kappa_R/\Omega_s)\partial_\tau A\,, \qquad (3)$$

where $\kappa_R = \mathrm{Re}\kappa$ is the real part of the eigenvalue with $\kappa_I < 0$. When z increases so that the growing perturbation is not much smaller than the soliton (nonlinear regime), the total field is no longer suitably described by $A = A_s + \delta A$ with δA in Eq. (2). However, the NSE can be seen to imply that the total field A continues to satisfy Eq. (3). To see this, we write, from the NSE, $\partial_z\partial_z A = \partial_z\mathcal{L}(A) + \partial_z[f(|A|^2)A] = \mathcal{L}(\partial_z A) + \{\partial_A[f(|A|^2)A]\partial_z A + \partial_{A^\star}[f(|A|^2)A]\partial_z A^\star\}$. At sufficiently small z, the weakly perturbed soliton $A_s + \delta A$ satisfies Eq. (3). Thus, making use of this relation for $\partial_z A$ at sufficiently small z, and of the linearity of $\mathcal{L}$, we obtain $\partial_z\partial_z A = \partial_z[i\alpha A - \kappa_I\epsilon\partial_\epsilon A - (\kappa_R/\Omega_s)\partial_\tau A]$ at small z, i.e., the derivatives of the left hand and right hand sides of Eq. (3) are also equal. An iterative procedure shows that the same is true for derivatives of any order with respect to z, evaluated at sufficiently small z, of the left and right hand sides of Eq. (3). The full nonlinear evolution described by the NSE with arbitrary $f(|A|^2)$ implies, in conclusion, that if Eq. (3) is satisfied at sufficiently small z, the same is true for all its derivatives at the same z, and this amounts to say (for regular enough A) that Eq. (3) continues to be valid at large propagation distances z. In other words, if at the small perturbation regime the envelope is given by $A = A_s + \delta A$, with δA in Eq. (2) [which satisfies Eq. (3)], at the large perturbation regime A satisfies also Eq. (3).

Thus the expression $A = F[r; \epsilon e^{-\kappa_I z}; \tau - (\kappa_R/\Omega_s)z]\exp(i\alpha z)$, which is the general solution of Eq. (3), describes the total field everywhere, $F(r; x_1; x_2)$ being an unspecified function. The development of instability may lead to different scenarios at large distances, as the formation of nonlinear bullets, long-lived pulsations, or radiative decay into a linear regime, depending on the sign of material dispersion and dimensionality With normal dispersion, the instability of strip solitons leads to their radiative linear decay [16]. The spatiotemporal dynamics of cylindrically symmetric self-guided light beams is also observed to decay into a linear state that is, moreover, essentially the same state for a broad range of experimental conditions leading to wave self-guiding (intensity, power, focusing mechanism), [6, 7] and therefore independent of the exact conditions exciting the unstable modes. Assuming here a linear decay, if $F[r; \epsilon e^{-\kappa_I z}; \tau - (\kappa_R/\Omega_s)z]$ becomes at large z independent of the uncontrolled seed ϵ of the growing perturbation (2), then it becomes also independent of x_1, and the envelope of the form $A = G[r; \tau - (\kappa_R/\Omega_s)z]\exp(i\alpha z)$, which represents a distortion-free linear wave. This wave preserves however the information about the nonlinear wave vector shift α of the soliton, and the velocity mismatch κ_R/Ω_s (with respect to a plane pulse at ω_0) dictated at the small perturbation regime. The dispersion relation of the wave $A = G[r; \tau - (\kappa_R/\Omega_s)z]\exp(i\alpha z)$ is given, from the linear Schrödinger equation, by

$$K_\perp(\Omega) = \left\{2k_0\left[-\alpha - (\kappa_R/\Omega_s)\Omega + k_0''\Omega^2/2\right]\right\}^{1/2}, \quad (4)$$

where $K_\perp = (k_x^2 + k_y^2)^{1/2}$ and Ω is the frequency (detuning from ω_0) of any plane-wave monochromatic constituent. The new frequencies Ω hopefully generated at the nonlinear stage of instability are then expected to lead at large z to a concentration of spectral energy about values of $K_\perp$ in Eq. (4). If $k_0'' > 0$, Eq. (4) is the hyperbolic dispersion curve of an X wave (or elliptic dispersion curve of a O wave if $k_0'' < 0$) propagating at a group velocity mismatch κ_R/Ω_s. The wave $A = G[r; \tau - (\kappa_R/\Omega_s)z]\exp(i\alpha z)$ results from a coherent superposition of Bessel beams $J_0[K_\perp(\Omega)r]\exp\{-i[K_\perp^2/(2k_0) - k_0''\Omega^2/2]z\}\exp(-i\Omega\tau)$ with axial wave numbers $k_0 - [K_\perp^2/(2k_0) - k_0''\Omega^2/2] = k_0 + \alpha + (\kappa_R/\Omega_s)\Omega$ varying linearly with Ω.

Though our analysis holds in the asymptotic limit $\epsilon \to 0$, our numerical simulations support its validity for finite (but small) values of ϵ. As an example, we consider a saturable Kerr medium with $f(|A|^2) = i(\omega_0 n_2/c)|A|^2/(1+\gamma|A|^2)$, where $n_2 > 0$ is the nonlinear refraction index, and $\gamma|A|^2 \ll 1$ is assumed. Numerical evaluation of the lowest-order bound state $A_s(r) = a(r)\exp(i\alpha z)$ yields $\alpha = 0.200 k_{\rm NL}$ for $\gamma I = 0.1$, where $k_{\rm NL} = \omega_0 n_2 I/c$, $I = a^2(0)$ is the peak intensity, and the radial profile $a(r)$ of Fig. 1(a). Temporal MI with $k_0'' < 0$ is known to end with the formation of nonlinear 3D bullets , so we address here the case with $k_0'' > 0$.

A long but straightforward linear MI analysis (see, e.g., [8]), shows that there exist two eigenvalues κ and $-\kappa^\star$ with negative imaginary part for each modulation frequency Ω_s. The unstable perturbation associated to κ is of the form (2), and that associated to $-\kappa^\star$ is obtained by replacing $(\kappa, u, v) \to (-\kappa^\star, v^\star, u^\star)$. Figures 1(b) and (c) show ϵu and ϵv for a selected Ω_s (see caption), with a seed ϵ such that the maximum amplitude of the perturbation is much smaller than that of the soliton.

To investigate the large perturbation regime and beyond, we solved numerically Eq. (1) with the initial condition $A(r, z=0, \tau) = A_s(r, z=0) + \delta A(r, z=0, \tau) = a(r) + \epsilon[u(r)\exp(-i\Omega_s\tau) + v^\star(r)\exp(\Omega_s\tau)]$, i.e., with the soliton plus the unstable perturbation (2) of eigenvalue κ at a modulation frequency Ω_s, which is so assumed to have been excited. Fig. 2 shows the initial condition (a) in (r, τ) space and (b) in Fourier space $(K_\perp, \Omega)$, where the sole three discrete frequencies $-\Omega_s, 0, +\Omega_s$ are conveniently displayed as three vertical strips.

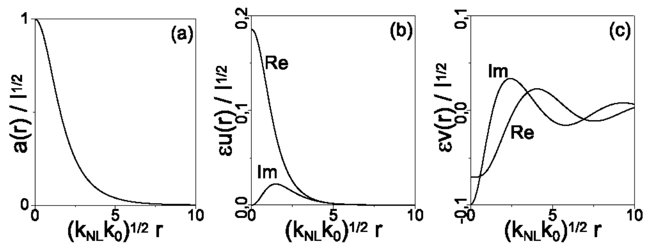

FIG. 1: (a) Profile $a(r)$ of the ground state of the NSE with saturable nonlinearity with $\gamma I = 0.1$. (b) and (c) Parts $\epsilon u(r)$ and $\epsilon v(r)$ of the unstable perturbation δA at modulation frequency $(k_0''/k_{\rm NL})^{1/2}\Omega_s = 0.628$, for which $\kappa = k_{\rm NL}(0.402 - i0.109)$. The seed ϵ is such that the perturbation is small (note the vertical scale changes).

Figure 2(g) shows the variation with z of the power carried by the different frequencies. The power in the modulation frequencies $\pm\Omega_s$ (dashed curve) grows first with the exponential gain predicted by the MI analysis (thin

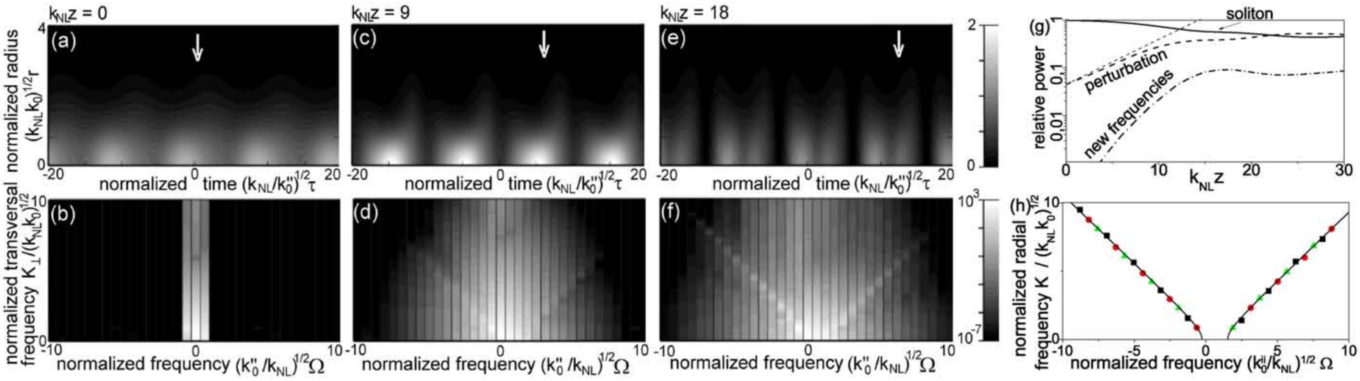

FIG. 2: For the initial condition in (a, b), gray scale plots at (c, d) $k_{\rm NL}z = 9$ and (e, f) $k_{\rm NL}z = 18$ of $|A(r,\tau)|^2$ (top) and $|A(K_\perp,\Omega)|^2$ (bottom). (g) Variation along z of the power in the soliton, perturbation and newly generated frequencies. (h) Solid curve: Expected final X-wave spectrum (4) for the soliton of Fig. 1(a) ($\alpha = 0.200k_{\rm NL}$) when modulated at $(k_0''/k_{\rm NL})^{1/2}\Omega_s = 0.628$. Squares, circles and triangles place the maxima of the long-distance spectrum for simulations with seeds ϵ ($k_{\rm NL}z = 18$), $\epsilon/2$ ($k_{\rm NL}z = 24$) and $\epsilon/4$ ($k_{\rm NL}z = 30$).

dashed line). When the soliton power loss (solid curve) is not negligible, exponential growth ceases. The nonlinear interaction between the soliton and the (no longer small) perturbation is seen to amplify new, multiple frequencies $\Omega = \pm N\Omega_s$, $N = \pm 2, \pm 3\ldots$ also exponentially (dash-dotted curve). At larger z, power exchange between the different frequencies ceases gradually, indicating a relaxation stage of the instability.

Figures 2 (c,d) and (e,f) correspond to the nonlinear and relaxation regimes, respectively. The generation of new frequencies results in the periodic break-up of the soliton into a train of pulses of repetition frequency Ω_s, each one developing the characteristic tails of X waves in space and time [Figs. 2(c) and (e)]. These exponentially emerging X waves could relate, in absence of linear relaxation, to the X-shaped shock fronts in the self-focusing of short pulses with pure Kerr nonlinearity. The arrow in Fig. 2, placed at times $\tau = (\kappa_R/\Omega_s)z$ for each z, is seen to move locked with the pulse train, evidencing that the latter travels at the predicted velocity mismatch κ_R/Ω_s. The spatiotemporal spectrum $(K_\perp,\Omega)$ of the pulse train at increasing z is shown in Figs. 2(d) and (f), and evidences the X-wave feature of the pulse train. The spectrum develops definite maxima at $K_\perp$ fitting to Eq. (4) for each new frequency $\Omega = \pm N\Omega_s$. The theoretical hyperbolic spectrum [Eq. (4)] with the value of α of this soliton, and Ω_s and κ_R of the initial weak perturbation, is shown in Fig. 2(h, solid curve) for comparison. Note the asymmetry of the spectrum with respect to $\Omega = 0$, with a branch passing close to $\Omega = 0$, as in many experiments and simulations [6, 7], and in contrast to the symmetric spectrum in the instability of plane waves. [9]. At longer z, the structure of the spectrum remains unchanged. The pure hyperbolic spectrum of infinite-energy X waves is never reached because of the finite energy in each temporal slice of the soliton. The X waves show indeed the typical quasi-nondiffracting behavior of X waves with finite energy.

The independence of the asymptotic hyperbolic spectrum of the seed ϵ of the weak perturbation in the initial condition is evidenced in Fig. 2(h). The maxima $K_\perp$ at diverse frequencies Ω in the simulated $(K_\perp,\Omega)$ spectrum at sufficiently long z are displayed for three values of the seed (ϵ, corresponding to (f), $\epsilon/2$ and $\epsilon/4$) in the initial condition. The maxima for all seeds fit well to the same hyperbolic spectrum of Eq. (4). As the seed is smaller, longer z is needed to reach the asymptotic spectrum, but the fitting to Eq. (4) is more accurate.

In conclusion, we have described a new type of break-up instability of cylindrically symmetric solitons into conical waves, which is expected to occur whenever the MI-driven spatiotemporal dynamics of the soliton decays into a linear state after its nonlinear stage of development.

J. Y. Lu and J. F. Greenleaf, IEEE Trans. Ultrason. Ferroelectr. Freq. Control **39,** 19 (1992).

H. E. Hernández-Figueroa, M. Zamboni-Rached, and E. Recami, Eds., *Localized Waves,* (Wiley, 2008).

S. Orlov, A. Piskarskas, and A. Stabinis, Opt. Lett. **27,** 2103 (2002).

C. Conti, S. Trillo, P. Di Trapani, G. Valiulis, A. Piskarskas, O. Jedrkiewicz, and J. Trull, Phys. Rev. Lett. **90,** 170406 (2003).

P. Di Trapani, G. Valiulis, A. Piskarskas, O. Jedrkiewicz, J. Trull, C. Conti, and S. Trillo, Phys. Rev. Lett. **91,** 093904 (2003).

D. Faccio, M.A. Porras, A. Dubietis, F. Bragheri, A. Couairon, and P. Di Trapani, Phys. Rev. Lett. **96,** 193901 (2006).

M. Kolesik, E. M. Wright, and J. V. Moloney, Opt. Express **13,** 10729-10741 (2005).

M. A. Porras, A. Parola, D. Faccio, A. Couairon, P. Di Trapani, Phys. Rev. A **76,** 011803(R) (2007).
C. Conti, Phys. Rev. E **68,** 016606 (2003).
C. Conti, Phys. Rev. E **70,** 046613 (2004).
V.E. Zakharov and A.M. Rubenchik, Sov. Phys. JETP **38,** 494-500 (1974).
D.E. Pelinovsky, Math. Compt. Simul. **55,** 585-594 (2001).
A.V. Yulin, D.V. Skryabin, and A.G. Vladimirov, Opt. Express **14,** 12347-12352 (2006). Phys. Rev. Lett. **99,** 223902 (2007).
A. De Rossi, S. Trillo, A. V. Buryak, and Y. S. Kivshar, Opt. Lett. 22, 868-870 (1997).
N. N. Akhmediev, V. I. Korneev, and R. F. Nabiev, Opt. Lett. **17,** 393-395 (1992).
S.P. Gorza, N. Roig, Ph. Emplit, and M. Haelterman, Phys. Rev. Lett. **92,** 084101 (2004).
L. Bergé, K. Germaschewski, R. Grauer, and J. Juul Rasmussen, Phys. Rev. Lett. **89,** 153902 (2002).